VNU Journal of Science: Mathematics - Physics

Journal homepage: https://js.vnu.edu.vn/MaP

Original Article

# Enhanced Photocatalytic Activity Using Near Visible Light of ZnO Nanorods by Doping with $Mn^{2+}$ Ions

Luong Hoai Nhan[1], Nguyen Huu Khoa[1], Lai Thi Ngoc Huyen[1], Huynh Hung Quang[1], Dinh Tan Muon[1], Nguyen Ngoc Phuong[4], Tran Cong Khanh[1,2], Phan Bach Thang[1,2,3], Dang Vinh Quang[1,2,3,*]

[1]*Department of Materials Science and Technology, University of Science, Nguyen Van Cu, District 5, Ho Chi Minh City, Vietnam*

[2]*Vietnam National University, Ho Chi Minh City (VNUHCM), Linh Trung, Thu Duc, Ho Chi Minh City, Vietnam*

[3]*Center for Innovative Materials and Architectures (INOMAR), Linh Trung, Thu Duc, Ho Chi Minh City, Vietnam*

[4]*Institute of Applied Materials Science (IAMS), Vietnam Academy of Science and Technology, TL29, Thanh Loc, District 12, Ho Chi Minh City, Vietnam*

Received 06 December 2020
Revised 01 January 2021; Accepted 01 January 2021

**Abstract:** ZnO is a promising photocatalyst for photocatalytic oxidation of organic compounds under the influence of sunlight that provides clean energy and decomposes sustainable organic pollutants substances. ZnO is found to have non-toxic properties, long-term stability, high carrier mobility, low cost and biocompatibility. However, some disadvantages of ZnO limit its use in photocatalysis. Due to its wide bandgap, ZnO can only be activated under UV illumination. On the other hand, the photo-excited electron-hole pairs that recombine quickly on ZnO surface, suppress its photocatalytic properties. To improve its properties and performance, doping with transition metals was used to improve the optical properties of ZnO. Among the transition metal ions, Manganese (Mn) was commonly used to improve and tune the optical, electrical, diameter, height, and the number of nanorods (NRs) per unit area. Introduction of Mn into ZnO could enhance the photocatalytic activity due to the increase in the defect sites that effectively decreased the recombination of free electrons and holes. This study successfully synthesized ZnO nanorod arrays

* Corresponding author.
*E-mail address:* vinhquangntmk@gmail.com

https//doi.org/10.25073/2588-1124/vnumap.4629

generated on glass substrates with different concentrations of doping Mn (0, 0.5, 1, 1.5 and 2%) at 100 °C by a simple hydrothermal method. To investigate the structure, morphology and optical properties, ultraviolet-visible spectroscopy (UV-Vis), X-ray diffraction (XRD) and scanning electron microscopy (SEM) were conducted. With the range of Mn doping ≤ 2% mol, the band gap reduced slightly, and the most optimized Mn doping concentration was of 0.5%. Overall, this work shows that the most effective way to increase ZnO's photocatalytic activity in the visible region by reducing its band gap was the reduction in the size of the material or denaturation of ZnO by certain metals or non-metals.

*Keywords:* ZnO NRs, doping, photocatalyst, visible light, methylene blue

## 1. Introduction

The rapid development of human society is making people suffer from environmental problems, such as air pollution, water pollution. Therefore, developing a non-polluting and environmentally friendly technology, as well as providing sustainable and clean energy have become an emerging task over the past few years. Semiconductor materials in the photocatalyst field are becoming more and more attractive and important because they contribute greatly to solve environmental problems such as waste water treatment and air purification [1-3]. These materials can produce electrons and holes which are highly active and capable of reducing pollutants in the water under illumination. Photocatalysts have many advantages including low-cost, low toxicity, low energy consumption, as well as low secondary pollution and reusability.

In this regard, catalytic oxidation technology attracts more and more attention. Among all photocatalytic materials, ZnO is a n-type semiconductor with a wide direct band (about 3.27 eV) which is widely used to remove pollutants in water. ZnO also has the non-toxic properties, long-term stability, high carrier mobility, low cost and biocompatibility [4]. However, some disadvantages of ZnO limit its application in photocatalysis. For instance, ZnO can only be activated under UV illumination due to its wide bandgap. On the other hand, the photo-excited electron quick recombination of the photo-excited electrons and holes on the ZnO surface that limits its photocatalytic properties. In order to handle these problems, doping with transition metals was used to improve the optical properties of ZnO and suppress the recombination of photo-generated charge carriers. Doping of transition metal ions, such as Mn, Al, Co and Cu into ZnO has been reported to reduce the bandgap energy and to prevent electron-hole pair recombination through the generation of new energy states [5-11]. With doping, the optical band gap value was decreased and the optical properties were improved [7, 12-15]. Among the transition metal ions, Manganese (Mn) was commonly used to improve the optical, electrical, diameter, height, and the number of nanorods (NRs) per unit area. Introduction of Mn ions into ZnO NRs could enhance the photocatalytic activity owing to the increase in the defect sites that effectively suppressed the recombination of free electrons and holes [16-18]. On the other hand, among the transition metals, ionic radius and covalent radius of $Mn^{2+}$ (0.8 Å and 1.17 Å) are close to $Zn^{2+}$ (0.74 Å and 1.25 Å). Therefore, $Mn^{2+}$ ions could easily replace $Zn^{2+}$ ions in the ZnO site without causing lattice deformation. Thus, Mn was a considerable candidate for doping into the ZnO matrix. However, there were few reports on visible light photocatalyst activity of Mn-doped ZnO NRs developed on substrates. Compared to other nanostructures, applying ZnO NRs on substrates for photocatalysis had such advantages as convenience for recycling and good reuse. The different concentrations of Mn doped into ZnO NRs were measured from the UV-Vis absorption spectra which showed the decrease in band gap upon Mn doping as expected. Mn-doped ZnO is the promising candidate which will be extensively researched.

Herein, Mn-doped ZnO NRs arrays were synthesized on glass substrates with different Mn concentrations by a simple hydrothermal method. 0.5% Mn concentration doping was optimized to reach the minimum optical band gap with the value of 3.175 eV for optoelectronic devices operating in the near visible radiations. More interestingly, the photocatalytic activities of undoped ZnO NRs and 0.5% Mn-doped ZnO NRs were investigated with MB at 10 ppm under 5W UV light. The degradation rate constant of device based on Mn-doped ZnO NRs was 32% higher than that in pure ZnO NRs with an increased value up to $1.32\ x\ 10^{-3}\ min^{-1}$.

## 2. Experiment

### *2.1. Material Chemicals and Characteristics*

ZnO NPs 40%.wt dispersion in ethanol, Zinc Nitrate Hexahydrate ($Zn(NO_3)_2.6H_2O$), Manganese (II) Chloride ($MnCl_2$), Hexamethylenetetramine ($C_6H_{12}N_4$) and Methylene Blue ($C_{16}H_{18}ClN_3S$) were purchased from Sigma Aldrich. All material chemicals were used without further purification. The crystalline structure was recorded using Xray diffraction (XRD, Bruker D8 advance) with Cu-K$\alpha$ radiation (λ~1.542 Å). The optical properties were investigated by UV-Vis spectra (JASCO V670). The morphology properties were measured using field emission scanning electron microscopy (FESEM, Hitachi S-4800).

### *2.2.. Synthesis of ZnO NRs and ZnO NRs Doping*

Undoped and Mn-doped ZnO NRs were synthesized directly onto glass substrates by hydrothermal method. First of all, the 2% ZnO nanoparticles were diluted in ethanol. Then, the nano-seeds were spin coated onto glass substrates at 2000 rpm in 30 secs. The samples were dried at 100 ℃ in 10 minutes. Secondly, the substrates with seed layer were dipped in growth solution at 90 ℃ in 3 hours. The growth solutions were prepared with the mixing of $Zn(NO_3)_2.6H_2O$ (0.05M), Hexamethylenetetramine $C_6H_{12}N_4$ (HMTA), DI water and Manganese (II) Chloride ($MnCl_2$) with different concentrations (0; 0.5; 1; 1.5; and 2 mol%). Finally, the samples were cleaned with DI water and dried at 100 ℃ in 30 mins.

### *2.3. Photocatalytic Activity Measurement*

The photocatalytic activity of the Mn-doped ZnO NRs sample was evaluated by the photodegradation of MB dye. Pure and doped ZnO samples were stirred in 20 ml of MB solution with 10 ppm initially in the dark condition for 1 hour to achieve an equilibrium adsorption state. The samples were then irradiated under 5W light with the wavelength of 400 nm for 90 minutes. The absorption spectra of Methylene Blue (MB) solutions were measured every 15 minutes by UV-Vis spectroscopy (JASCO V670 machine).

## 3. Results and Discussion

### *3.1. Morphological and Structural Analysis*

Figures 1a, b, c show the top view SEM images of ZnO NRs doped with Mn at 0%, 0.5% and 2%. All the samples show that ZnO generally grew perpendicular to the surface of the glass substrate in the form of hexagonal structure [17, 19]. The average diameter of the NRs increased with the addition of Mn. Specifically, undoped ZnO NRs had an average diameter of 66.9 nm, 0.5% Mn-doped ZnO NRs

had an average diameter of 70.9 nm, and 2% Mn-doped ZnO NRs had an average diameter of 88.9 nm. The cross-sectional images of the Mn-doped ZnO NRs in Figures 1 d, e, f show that the average height increased in the Mn concentration. The average lengths of the ZnO NRs with 0, 0.5 and 2% Mn concentrations were 0.799, 0.893 and 1.05 μm, respectively. The effect of doping Mn on the morphology of ZnO NRs was also presented in the previous reports [17, 20]. For example, the 5 mol% Mn doped into ZnO NRs increased the diameter of the NRs from 85 to 150 nm and 2 at% Mn increased the diameter range of ZnO NRs from 120-400 nm to 120-700 nm [21]. The enhancement of ZnO crystal growth may be created by doping Mn elements. The evidence was the increase in the diameter, length, and the number of NRs per unit area, which resulted in the increase in the ZnO surface area shown in these SEM [22].

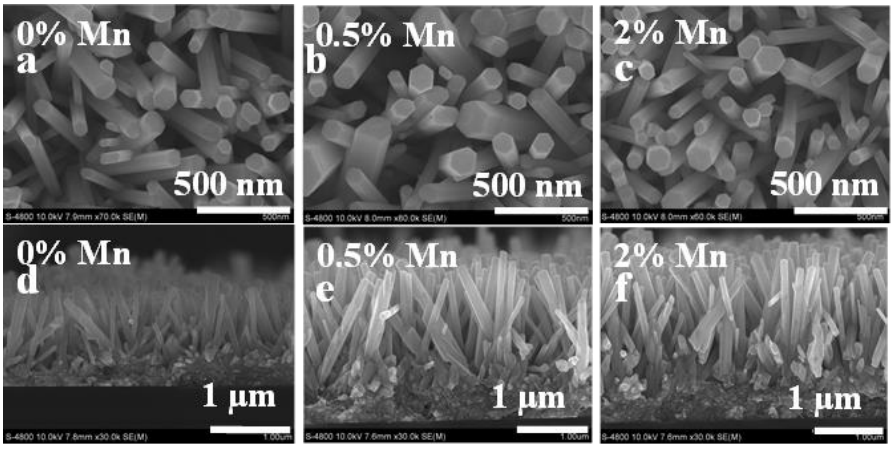


Figure 1. The SEM images of ZnO:Mn NRs at 0%, 0.5%, and 2% doping concentrations.
a, b, c - Top view and d, e, f - Cross-section.

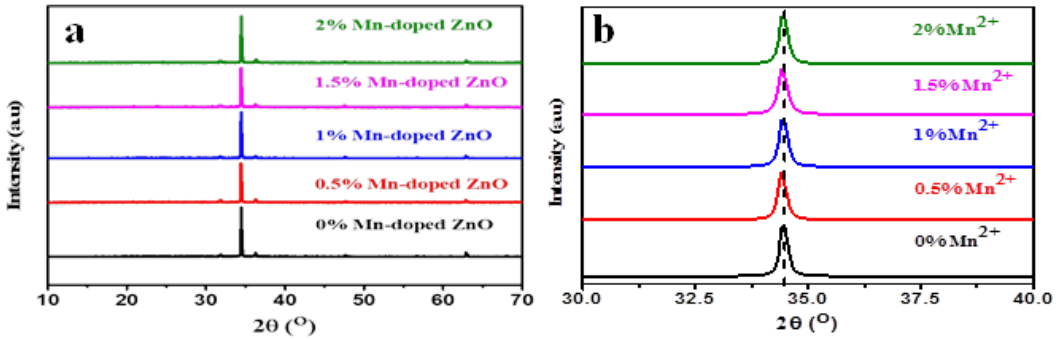


Figure 2. a. XRD patterns of the undoped and Mn-doped ZnO NRs at different concentrations;
b. The large scale of (0.02) peak.

The crystalline structures of the undoped ZnO and Mn-doped ZnO NRs were studied from the XRD patterns. Figure 2a presents the XRD peaks characterizing the hexagonal wurtzite structure of ZnO materials with a preferential orientation along the c-axis. All the diffraction peaks at angles $2\theta = 31.8$, 34.5, 36.3, 47.6 and 62.3 correspond to the reflection from the (100), (002), (101), (102) and (103) crystal planes. No stranger peaks are observed in XRD patterns that demonstrate the good substitution of $Mn^{2+}$ ions for $Zn^{2+}$ ions in crystal lattice, i.e., Mn ions successfully doped into ZnO NRs without any

degradation. Figure 2b shows the highest peak at (002) plane of pure and Mn-doped ZnO NRs, which indicates the preferred orientation of NRs. The average crystallite size 'D' of the samples was calculated using the Debye - Scherrer formula [23], $D = \frac{k\lambda}{\beta_{hkl}.cos\theta}$, where λ was the wavelength of X-ray (1.5406 Å), $\beta_{hkl}$ was the full-width at half-maximum in radian, and θ was the angle of diffraction. With the increase of Mn doping concentration from 0 to 2%, the crystalline size significantly increased from 64.303 to 82.823 nm due to the different ionic radius. More interestingly, the position of (002) peaks shifted toward the lower angle that was caused by the deformation of ZnO lattice. It was attributed to the larger ionic radius of $Mn^{2+}$ (0.80 Å) than that of $Zn^{2+}$ (0.74 Å) [17, 23-25].

*3.2. Optical Properties*

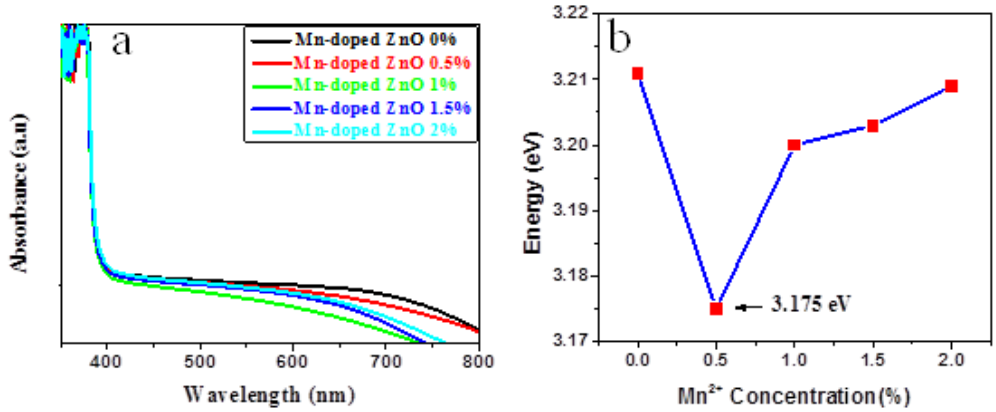


Figure 3. a. Absorbance spectra of Mn-doped ZnO NRs with different concentrations; b. The dependence of optical band gap on $Mn^{2+}$ concentration.

Figure 3a shows the optical absorbance spectra of ZnO NRs with different Mn doping concentrations. All samples exhibit a strong absorption in the ultraviolet region and weak absorption for the visible light. ZnO NRs displayed a sharp absorption edge at a wavelength around 390 nm, which correlated with the value of the ZnO bandgap. Absorption band edge was observed at 390 nm for pure ZnO NRs. For Mn-doped ZnO NRs, the absorption edge shifted toward the long wavelength as well as the visible light. It was attributed to the narrow optical band gap due to the presence of Mn energy level located inside the ZnO NRs band gap. The optical bandgap of all the samples could be estimated according to the Tauc's method, $\alpha h\nu = (h\nu - E_g)^n$, where α was the optical absorption coefficient, h was the Planck constant, $\nu$ was the photon frequency, $E_g$ was the optical band gap and n was a parameter associated with the type of electronic transition: n = 1 for the direct semiconductor (for example ZnO, ZnS) and n = 2 in the indirect semiconductor. The value of band gap ($E_g$) could be estimated by extrapolating the linear portion of the plot $(\alpha h\nu)^2$ versus $h\nu$ to $(\alpha h\nu)^2 = 0$. Figure S1 supporting information clearly shows the calculation of the optical band gap of pure ZnO NRs and doped ZnO NRs through Tauc's method. The optical band gap of pure ZnO NRs and doped ZnO NRs with 0.5%, 1%, 1.5% and 2% Mn were 3.175, 3.1989, 3.203 and 3,209 eV corresponding to optical absorption region with wavelength ≤ 391, ≤ 388, ≤ 387 and ≤ 386 nm. The characteristic research results show that un-doped ZnO NRs and Mn-doped ZnO NRs materials were successfully synthesized by hydrothermal method. The materials were nanometer-sized and had the ability to absorb near-visible light. Figure 3b shows that the lowest optical band gap was observed at 0.5% Mn-doped ZnO NRs with the value of 3.175 eV. The decrease of the optical bandgap originated from the optically activated sub-levels formed

by doping. This can be explained by the interaction between the d electron of an Mn atom and the s and p electrons of the host Zn atom (s–d and p–d interactions) that formed the new energy levels[20, 26-28]. Furthermore, the decrease in optical band gap under doping was explained by the presence of crystal defects, such as oxygen vacancies [30, 31]. However, with the further increase of Mn concentration (0.5% to 2%), the optical band gap was increased (3.175 eV to 3.209 eV). This may be attributed to the structural changes of ZnO owing to $Mn^{2+}$ doping [32]. However, we assumed that more MnOx could be formed by the reaction between Oxygen and Mn at high dopant concentration $Mn^{2+}$ instead of taking interstitial or substitutional site in ZnO crystal. The doping of ZnO with $Mn^{2+}$ added the tail states in the vicinity of the valence band owing to the defect sites and reduced its effective band gap. This decrease in the band gap [33], which subsequently caused the red shift in the optical absorption of $Mn^{2+}$doped ZnO nano/microfilms [34] and nanoparticles [32] had been reported for lower dopant concentration.

### *3.3. Photocatalytic Activities*

The degradation of MB was observed by recording the decrease in optical absorption peak at 660.5 nm with increasing time of light irradiation (Figures 4 a-f). The optical absorption spectra were carried out using UV–vis spectroscopy. The photocatalytic activities of all five as-synthesized samples were studied by following the discoloration of their respective MB solutions under near visible light irradiation. To evaluate photocatalytic activity of ZnO and Mn-doped ZnO NRs, degradation of MB was studied. The measurement system was set up as Figure S2. Under the near visible light exposure, the decreases of absorption peak intensities at 660.5 nm of MB were neglected (Figure 4a), while these decreases were observed in the samples with catalyst (Figures 4 b-f). The highest decrease of absorption peaks was presented in the sample based on 0.5% Mn-doped ZnO NRs. The photocatalytic efficiency for the MB degradation was determined by using the following equation, $Degradation\,(\%) = \frac{C_o - C_t}{C_o}\ x\ 100$, where Co (ppm) was the initial concentration of MB and Ct (ppm) was the concentration of MB at certain reaction time t (min).

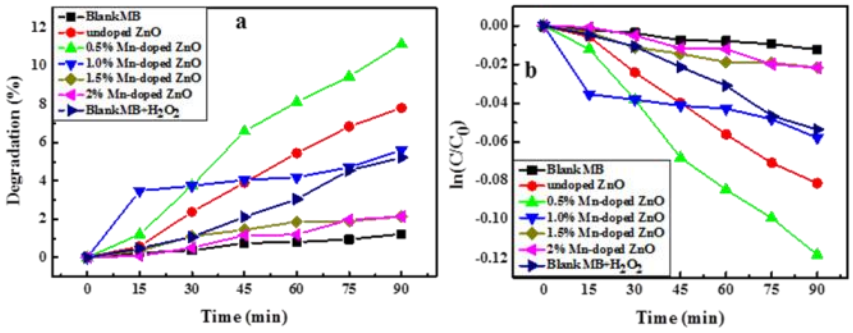


Figure 4. Absorbance spectra of MB: a. MB without catalyst; MB and catalyst follow the increasing of $Mn^{2+}$ doping concentration; b. 0%; c. 0.5%; d. 1%; e. 1.5%; and f. 2%.

The degradation of MB under near visible irradiation with the presence of different catalysts was shown in Figure 5a. For comparison, blank experiments without catalysts were also performed. The fastest degradation of MB belonged to the catalyst with 0.5% Mn-doped ZnO NRs after light exposure for 90 minutes. Besides, we also investigated the optical decomposition ability of MB in the presence of $H_2O_2$ which had the effect of creating many hydroxyl radicals and reducing MB dye. The MB sample

with $H_2O_2$ showed that $k_{app}$ value ($5.63\ x\ 10^{-4}.min^{-1}$) was much larger than that in the sample without $H_2O_2$, indicating that $H_2O_2$ was added to remove MB under light exposure [35]. As shown in Figure 5a, for the samples without any catalysts, MB was slightly degraded under light illumination. The efficiency deteriorates with the presence of 7.8% pure ZnO sample after 90 minutes illumination of near visible light. When Mn-doped ZnO NRs was used as a catalyst, the catalytic effect was much improved in the same situation. The ZnO sample doped with 0.5% Mn shows the highest photochemical catalyst efficiency, reducing MB by 11.14% for 90 minutes. Besides, the photocatalytic performance was calculated by the equation $\ln\left(\frac{C}{C_o}\right) = -k_{app}t$, where $C_o$ represented the initial MB concentration, C stood for its concentration at any time t of the photo irradiation, and k was the first-ordered degradation rate constant. The results of the tests were given in Figure 5b. When suitable Mn ions were doped, Mn sites could promote charge separation. However, excessive Mn doping could yield crystal defects, which would serve as the center of recombination of shaped pairs of electron holes. Therefore, the separation of charge was inhibited and photocatalytic activity decreased [24, 31].

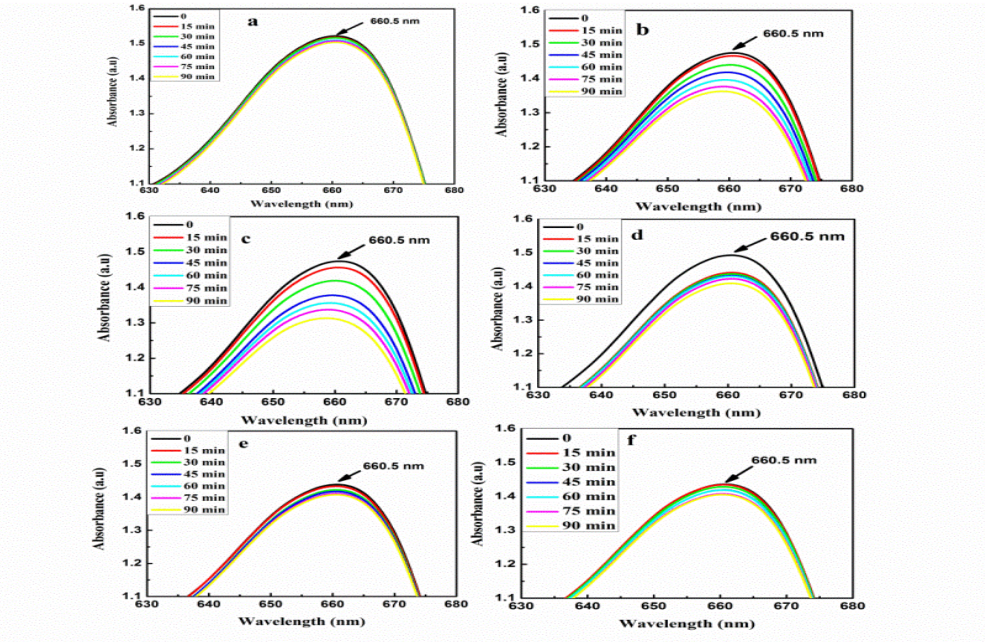


Figure 5. a. Photocatalytic degradation under near visible light by Mn-doped ZnO NRs; b. Ln vs t plot for different catalyst loads.

Table 1. $k_{app}$ and $R^2$ of photocatalyst activities.

| | **$k_{app}$ ($10^{-3}$.min$^{-1}$)** | **$R^2$** |
|---|---|---|
| Blank | 0.1363 | 0.991 |
| Blank-$H_2O_2$ | 0.563 | 0.982 |
| 0% Mn-doped ZnO NRs | 1.0 | 0.9944 |
| 0.5% Mn-doped ZnO NRs | 1.34 | 0.9952 |
| 1% Mn-doped ZnO NRs | 0.684 | 0.981 |
| 1.5% Mn-doped ZnO NRs | 0.271 | 0.977 |
| 2% Mn-doped ZnO NRs | 0.237 | 0.978 |

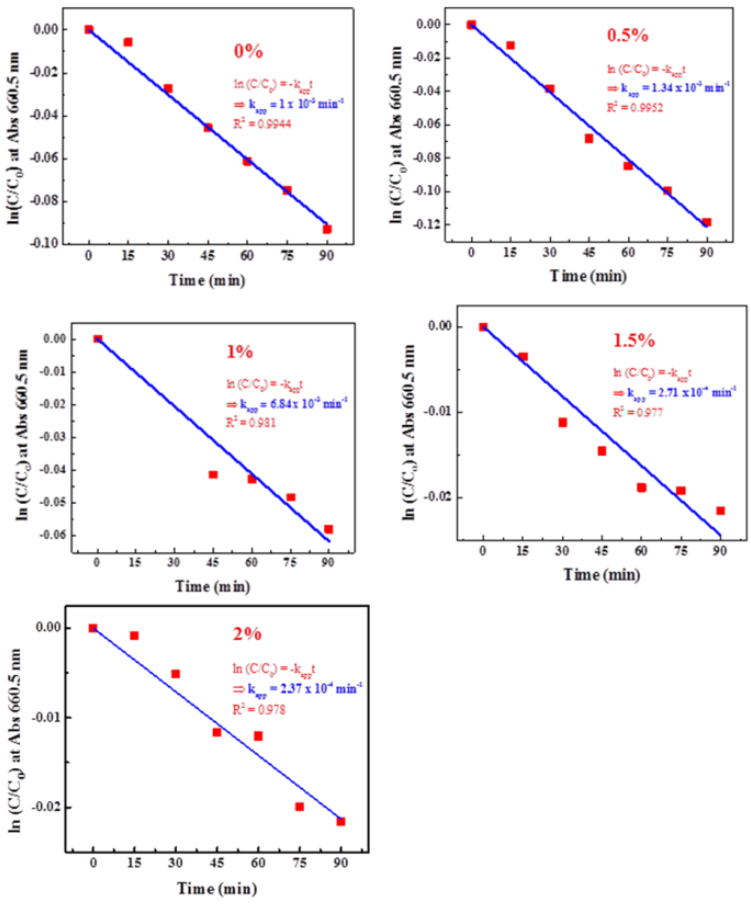


Figure 6. Degradation ratio constant of Mn-doped ZnO NRs with different concentrations.

To better understand the photocatalytic performance, the degradation ratio constants of devices based on ZnO NRs doped with different Mn concentrations were exhibited in Figure 6. The MB degradation rate constant ($k_{app}$) of ZnO:Mn samples was higher than that of pure ZnO NRs. When the Mn doping concentration was 0.5%, $k_{app}$ of MB treatment increased from $1.0\,x\,10^{-3}.min^{-1}$ to $1.34\,x\,10^{-3}.min^{-1}$ . However, when Mn concentration was further increased, the MB treatment efficiency decreased from $1.34\,x\,10^{-3}.min^{-1}$ to $2.4\,x\,10^{-4}.min^{-1}$ at 90-minute photo irradiation. These results are presented in Figure 6 and Table 1. So ZnO doped with 0.5% Mn reached the highest photocatalytic activity. These results could be explained as follows, when the concentration of Mn doping increased, $Mn^{2+}$ ions would replace $Zn^{2+}$ ion position in the hexagonal structure of ZnO, creating point defects due to strange ions in the structure of ZnO. It was the formation of these defects that reduced the band gap of the material. But when the concentration of $Mn^{2+}$ doping was increased further to a certain value (greater than 0.5% in molar ratio), it was possible that oxidation reactions forming Mn oxides ($Mn_xO_y$) on ZnO surface interfered with ZnO's light absorption process leading to the reduced photocatalytic activity of ZnO. On the other hand, because the $Mn^{2+}$ ion radius was 0.80 Å greater than the $Zn^{2+}$ ion radius by 0.74 Å, the replacement of many $Mn^{2+}$ ions in ZnO structure could change the hexagonal structure of ZnO, this was mentioned in Pauling's rule, concluding that Mn could replace Zn without changing the structure. From these results, we found that 0.5% Mn-doped ZnO NRs had the

highest photocatalytic activity [18]. The improved photocatalytic efficiency of catalysts evaluated in terms of degradation ratio constant of dye could be attributed to three factors. Firstly, Mn elements may have induced an enhancement of ZnO surface area, as evidenced by the increase in the diameter, height, and number of NRs per unit area, as shown in the SEM images. Meanwhile, the ZnO wurtzite structure was well-preserved, even when the crystallite size increased, as indicated by the XRD spectra. This morphological effect considerably increased the surface area of the ZnO and hence the generation of free electrons and holes for photodegradation of MB dye molecules were enhanced [20, 36, 37]. Secondly, Mn elements may have led to the narrowing of band gap that was favorable for photoexcitation of more electrons from valence band to conduction band as demonstrated in the UV-Vis spectra (Figure 3). Lastly, the Mn elements may have induced the increase of the number of oxygen vacancies, as indicated by the decrease in the lattice constants, the increase in the A1 (low) peak in the Raman spectra, and the visible light emission, as was reported by Putri et al., [16]. These crystal defects were also well known to inhibit the recombination process of electrons and free holes because $Mn^{2+}$ ions could act as electron traps or intermediate steps. Donkova et al., [38] reported that these doping ions would shift the Fermi level up to the bottom edge of the conduction band, which would increase the adsorption ability to the oxygen [38]. This synergistic effect actually depended on the Mn content in the ZnO because some reports indicated the opposite effect if the Mn content was not optimum.

### *3.4. Photocatalytic Mechanism*

The photocatalytic mechanism was explained by absorbed and removal process. Firstly, the organic pollutants diffused from the liquid phase to the catalytic materials surface and the organic pollutants were adsorbed onto the surface. Next, under light exposure, oxidation and reduction reaction happened on the adsorbed phase. Lastly, the final products from the reaction process were desorbed and removed from the interface region [39]. The redox reaction occurring during photocatalysis was illustrated in Figure 7. Indeed, the doping of $Mn^{2+}$ was able to modify the energy band structure of ZnO by introducing impurity energy levels within the bandgap of ZnO [16, 40, 41]. The photo-generated electrons in the valence band of ZnO moved towards impurity energy levels or the conductor band and produced a large number of superoxide radicals ($O•^{2-}$) under the visible light irradiation, accompanied by the d-d transitions between the impurity energy levels. Meanwhile, the photo-excited holes were left behind in the ZnO valence band and moved to the surface of doped ZnO NRs, forming highly oxidative hydroxyl radical species (OH•) after reacting with water molecules [21]. $ZnO + h\nu \rightarrow e^{-}(CB) + h^{+}(VB)$. The electron-hole pairs could migrate to the ZnO surface and be involved in redox reactions: [21, 39].

$$e^{-} + O_2 \rightarrow ZnO + O•^{2-}$$

$$h^{+} + OH^{-} \rightarrow OH•$$

Then, the resulting hydroxyl radicals, which were powerful oxidizing agents, would attack the pollutants adsorbed on the surface of doped ZnO NRs to rapidly produce intermediate compounds. Intermediates would eventually be converted to less toxic compounds such as $CO_2$, $H_2O$ and mineral acids: [21, 39].

OH• + MB (Dye) → degradation products

O2•− + MB (Dye) → degradation products

Degradation products + OH• → Intermediates

Intermediates → $CO_2$ +$H_2O$

Therefore, less energy was needed to excite electrons from the valence band, resulting in an improvement in the absorption ability of ZnO NRs to visible light leading to enhance the photocatalytic activities. This proves that the optical bandgap was narrowed through $Mn^{2+}$ ion doping. Besides, the

doped $Mn^{2+}$ ions were also served as electronic traps. These trapping sites could restrict the recombination of photo-excited electron-hole pairs and promote the separation of photo-generated charge carriers. These things led to an enhancement in the photocatalytic activity of doped ZnO NRs under visible light.

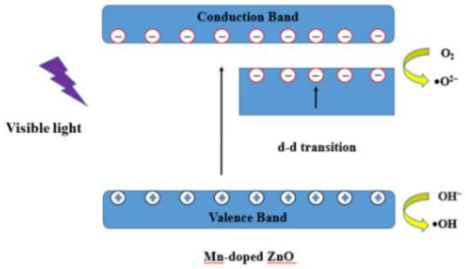


Figure 7. The photocatalytic mechanism of Mn-doped ZnO NRs.

## 4. Conclusion

Mn-doped ZnO NRs were successfully synthesized on glass substrates by hydrothermal method. The incorporation of $Mn^{2*}$ ions into ZnO crystal lattice was demonstrated through XRD pattern. The optical band gap was optimized with the minimum value of 3.175 eV at 0.5% Mn doping. The narrowing band gap led to a shift of the absorbed edge toward visible region. Under visible light illumination, the generated electron-hole pairs in Mn-doped ZnO NRs were higher than that in pure ZnO NRs, which improved the photocatalytic activities. Besides, the enhancement of oxygen vacancy concentrations played a significant role in inhibiting the recombination of free electrons and holes by trapping the excited electrons. The degradation MB based on ZnO:Mn NRs enabled the new potential applications, especially, the optoelectronic devices using visible light.

## Acknowledgements

This research was funded by Vietnam National University, Ho Chi Minh City (VNU-HCM) under Grant C2020-18-20.

## References

[1] J. Liqiang, F. Honggang, W. Baiqi, W. Dejun, X. Baifu, L. Shudan, S. Jiazhong, Effects of Sn Dopant on the Photoinduced Charge Property and Photocatalytic Activity of TiO2 Nanoparticles, Applied Catalysis B: Environmental, Vol. 62, No. 3, 2006, pp. 282-291, https://doi.org/10.1016/j.apcatb.2005.08.012.

[2] G. Cai, L. Xu, B. Wei, J. Che, H. Gao, W. Sun, Facile Synthesis of β-Bi2O3/Bi2O2CO3 Nanocomposite with High Visible-light Photocatalytic Activity, Materials Letters, Vol. 120, 2014, pp. 1-4, https://doi.org/10.1016/j.matlet.2014.01.027.

[3] Z. Muslim, K. Aadim, R. Kadhim, Preparation of ZnO for Photocatalytic Activity of Methylene Blue Dye, International Journal of Basic and Applied Science, Vol. 6, No. 1, 2017, pp. 1-7, https://doi.org/10.17142/ijbas-2017.6.1.1.

[4] Ü. Özgür, Y. I. Alivov, C. Liu, A. Teke, M. A. Reshchikov, S. Doğan, V. Avrutin, S. J. Cho, H. Morkoç, A Comprehensive Review of ZnO materials and Devices, Journal of Applied Physics, Vol. 98, No. 4, 2005, pp. 041301, https://doi.org/10.1063/1.1992666.

[5] F. Achouri, S. Corbel, L. Balan, K. Mozet, E. Girot, G. Medjahdi, M. B. Said, A. Ghrabi, R. Schneider, Porous Mn-doped ZnO Nanoparticles for Enhanced Solar and Visible Light Photocatalysis, Materials & Design. C, Vol. 101, 2016, pp. 309-316, https://doi.org/10.1016/j.matdes.2016.04.015.

[6] S. Anandan, A. Vinu, T. Mori, N. Gokulakrishnan, P. Srinivasu, V. Murugesan, K. Ariga, Photocatalytic Degradation of 2,4,6-trichlorophenol using Lanthanum Doped ZnO in Aqueous Suspension, Catalysis Communications - CATAL COMMUN, Vol. 8, No. 9 2007, pp. 1377-1382, https://doi.org/10.1016/j.catcom.2006.12.001.

[7] S. A. Ahmed, Structural, Optical, and Magnetic Properties of Mn-doped ZnO Samples, Results in Physics, Vol. 7, 2017, pp. 604-610, https://doi.org/10.1016/j.rinp.2017.01.018.

[8] R. Saleh, N. F. Djaja, Transition-metal-doped ZnO Nanoparticles: Synthesis, Characterization and Photocatalytic Activity under UV Light, Spectrochim Acta A Mol Biomol Spectrosc, Vol. 130, 2014, pp. 581-590, https://doi.org/10.1016/j.saa.2014.03.089.

[9] N. Verma, S. Bhatia, R. K. Bedi, Sn-doped ZnO Nanopetal Networks for Efficient Photocatalytic Degradation of Dye and Gas Sensing Applications, Applied Surface Science, Vol. 407, 2017, pp. 495-502, https://doi.org/10.1016/j.apsusc.2017.02.205.

[10] A. Tabib, W. Bouslama, B. Sieber, A. Addad, H. Elhouichet, M. Férid, R. Boukherroub, Structural and optical Properties of Na Doped ZnO Nanocrystals: Application to Solar Photocatalysis, Applied Surface Science, Vol. 396, 2017, pp. 1528-1538, https://doi.org/10.1016/j.apsusc.2016.11.204.

[11] A. Kadam, D. D. Bhopate, V. Kondalkar, S. Majhi, C. Bathula, A. V. Tran, S. W. Lee, Facile Synthesis of Ag-ZnO Core–shell Nanostructures with Enhanced Photocatalytic Activity, Journal of Industrial and Engineering Chemistry, Vol. 107, 2017, pp. 2411-2502, https://doi.org/10.1016/j.jiec.2017.12.003.

[12] N. Kamarulzaman, M. F. Kasim, R. Rusdi, Band Gap Narrowing and Widening of ZnO Nanostructures and Doped Materials, Nanoscale Research Letters, Vol. 10, No. 1, 2015, pp. 346, https://doi.org/10.1186/s11671-015-1034-9.

[13] A. S. Hameed, C. Karthikeyan, S. Sasikumar, V. S. Kumar, G. Ravi, Impact of Alkaline Metal Ions $Mg^{2+}$, $Ca^{2+}$, $Sr^{2+}$ and $Ba^{2+}$ on the Structural, Optical, Thermal and Antibacterial Properties of ZnO Nanoparticles Prepared by the Co-Precipitation Method, Journal of Materials Chemistry B, Vol. 1, No. 43, 2021, pp. 5950-5962, http://doi.org/10.1039/C3TB21068E.

[14] D. Appell, Nanotechnology, Wired for Success, Nature, Vol. 419, No. 6907, 2002, pp. 553-555, https://doi.org/10.1038/419553a.

[15] D. P. Joseph, C. Venkateswaran, Bandgap Engineering in ZnO By Doping with 3d Transition Metal Ions, Journal of Atomic and Molecular Physics, Vol. 2011, 2011, pp. e270540, https://doi.org/10.1155/2011/270540.

[16] N. A. Putri, V. Fauzia, S. Iwan, L. Roza, A. A. Umar, S. Budi, Mn-doping-induced Photocatalytic Activity Enhancement of ZnO Nanorods Prepared on Glass Substrates, Applied Surface Science, Vol. 439, 2018, pp. 285-297, https://doi.org/10.1016/j.apsusc.2017.12.246.

[17] N. Rajamanickam, S. Rajashabala, K. Ramachandran, Effect of Mn-doping on the Structural, Morphological and Optical Properties of ZnO Nanorods, Superlattices and Microstructures, Vol. 65, 2014, pp. 240-247, https://doi.org/10.1016/j.spmi.2013.11.005.

[18] S. Senthilkumaar, K. Rajendran, S. Banerjee, T. K. Chini, V. Sengodan, Influence of Mn Doping on the Microstructure and Optical Property of ZnO, Materials Science in Semiconductor Processing, Vol. 11, No. 1, 2008, pp. 6-12, https://doi.org/10.1016/j.mssp.2008.04.005.

[19] J. Du, Z. Liu, Y. Huang, Y. Gao, B. Han, W. Li, G. Yang, Control of ZnO Morphologies Via Surfactants Assisted Route in the Subcritical Water, Journal of Crystal Growth, Vol. 280, No. 1-2, 2005, pp. 126-134, https://doi.org/10.1016/j.jcrysgro.2005.03.006.

[20] M. Yilmaz, Ş. Aydoğan, The Effect of Mn Incorporation on the Structural, Morphological, Optical, and Electrical Features of Nanocrystalline ZnO Thin Films Prepared by Chemical Spray Pyrolysis Technique, Metallurgical and Materials Transactions A, Vol. 46, No. 6, 2015, pp. 2726-2735, https://doi.org/10.1007/s11661-015-2875-7.

[21] W. Li, G. Wang, C. Chen, J. Liao, Z. Li, Enhanced Visible Light Photocatalytic Activity of ZnO Nanowires Doped with Mn2+ and Co2+ Ions, Nanomaterials (Basel), Vol. 7, No. 1, 2017, pp. E20, https://doi.org/10.3390/nano7010020.

[22] B. Panigrahy, M. Aslam, D. Bahadur, Aqueous Synthesis of Mn- and Co-Doped ZnO Nanorods, J. Phys. Chem. C, Vol. 114, No. 27, 2010, pp. 11758-11763, https://doi.org/10.1021/jp102163b.

[23] U. Holzwarth, N. Gibson, The Scherrer Equation Versus the "Debye-Scherrer equation," Nature Nanotech, Vol. 6, 2011, pp. 534-534, https://doi.org/10.1038/nnano.2011.145.

[24] Q. Ma, X. Lv, Y. Wang, J. Chen, Optical and Photocatalytic Properties of Mn Doped Flower-like ZnO Hierarchical Structures, Optical Materials, Vol. C, 2016, pp. 86-93, https://doi.org/10.1016/j.optmat.2016.07.014.

[25] M. V. Gallegos, M. A. Peluso, H. Thomas, L. C. Damonte, J. E. Sambeth, Structural and Optical Properties of ZnO and Manganese-doped ZnO, Journal of Alloys and Compounds, Vol. 689, 2016, pp. 416-424, https://doi.org/10.1016/j.jallcom.2016.07.283.

[26] Ş. Ş. Türkyılmaz, N. Güy, M. Özacar, Photocatalytic Efficiencies of Ni, Mn, Fe and Ag Doped ZnO Nanostructures Synthesized by Hydrothermal Method: The Synergistic/Antagonistic Effect between ZnO and Metals, Journal of Photochemistry and Photobiology A: Chemistry, Vol. 341, 2017, pp. 39-50, https://doi.org/10.1016/j.jphotochem.2017.03.027.

[27] V. V. Strelchuk, A. S. Nikolenko, O. F. Kolomys, S. V. Rarata, K. A. Avramenko, P. M. Lytvyn, P. Tronc, C. O. Chey, O. Nur, M. Willander, Optical and Structural Properties of Mn-doped ZnO Nanorods Grown by Aqueous Chemical Growth for Spintronic Applications, Thin Solid Films, Vol. 601, 2016, pp. 22-27, https://doi.org/10.1016/j.tsf.2015.11.019.

[28] P. Singh, A. Kaushal, D. Kaur, Mn-doped ZnO Nanocrystalline thin Films Prepared by Ultrasonic Spray Pyrolysis, Journal of Alloys and Compounds, Vol. 471, No. 1-2, 2009, pp. 11-15, https://doi.org/10.1016/j.jallcom.2008.03.123.

[29] L. C. Chen, C. H. Tien, C. S. Fu, Magneto-optical Characteristics of Mn-doped ZnO Films Deposited by Ultrasonic Spray Pyrolysis, Materials Science in Semiconductor Processing, Vol. 15, No. 1, 2012, pp. 80-85, https://doi.org/10.1016/j.mssp.2011.04.003.

[30] M. M. Cortalezzi, J. Rose, E. Tsui, A.R. Barron, J. Y. Bottero, M. Wiesner, Synthesis and Characterization of Manganese Doped Ferroxane Nanoparticles, MRS Proceedings, Vol. 800, 2003, pp. 27-32, https://doi.org/10.1557/PROC-800-AA9.4.

[31] R. Ullah, J. Dutta, Photocatalytic Degradation of Organic Dyes with Manganese-doped ZnO Nanoparticles, Journal of Hazardous Materials, Vol. 156, No. 1, 2008, pp. 194-200, https://doi.org/10.1016/j.jhazmat.2007.12.033.

[32] R. Viswanatha, S. Sapra, S. Sen Gupta, B. Satpati, P. V. Satyam, B. N. Dev, D. D. Sarma, Synthesis and Characterization of Mn-Doped ZnO Nanocrystals, J. Phys. Chem. B, Vol. 108, 2004, pp. 6303-6310, https://doi.org/10.1021/jp049960o.

[33] Z. B. Bahşi, A. Y. Oral, Effects of Mn and Cu Doping on the Microstructures and Optical Properties of Sol-Gel Derived ZnO thin Films, Optical Materials, Vol. 29, 2007, pp. 672-678, https://doi.org/10.1016/j.optmat.2005.11.016.

[34] U. N. Maiti, P. K. Ghosh, S. Nandy, K. K. Chattopadhyay, Effect of Mn Doping on the Optical and Structural Properties of ZnO Nano/micro-fibrous thin Film Synthesized by Sol–gel Technique, Physica B: Condensed Matter, Vol. 387, No. 1, 2007, pp. 103-108, https://doi.org/10.1016/j.physb.2006.03.090.

[35] Z. B. Bahşi, A. Y. Oral, Effects of Mn and Cu Doping On The Microstructures And Optical Properties of Sol–Gel Derived ZnO thin Films, Optical Materials, Vol. 29, 2007, pp. 672-678, https://doi.org/10.1016/j.optmat.2005.11.016.

[36] M. Samadi, M. Zirak, A. Naseri, E. Khorashadizade, A. Z. Moshfegh, Recent Progress on Doped ZnO Nanostructures for Visible-light Photocatalysis, thin Solid Films, Vol. 387, No. 1, 2007, pp. 103-108, https://doi.org/10.1016/j.tsf.2015.12.064.

[37] D. K. Dubey, D. N. Singh, S. Kumar, C. Nayak, P. Kumbhakar, S. N. Jha, D. Bhattacharya, A. K. Ghosh, S. Chatterjee, Local Structure and Photocatalytic Properties of Sol-gel Derived Mn–Li Co-doped ZnO Diluted Magnetic Semiconductor Nanocrystals, RSC Advances, Vol 6, 2016, pp. 22852-22867, https://doi.org/10.1039/C5RA23220A.

[38] B. Donkova, D. Dimitrov, M. Kostadinov, E. Mitkova, D. Mehandjiev, Catalytic and Photocatalytic Activity of Lightly Doped Catalysts M:ZnO (M=Cu, Mn), Materials Chemistry and Physics, Vol. 123, No. 2, 2010, pp. 563-568, https://doi.org/10.1016/j.matchemphys.2010.05.015.

[39] C. B. Ong, L. Y. Ng, A. W. Mohammad, A review of ZnO Nanoparticles as Solar Photocatalysts: Synthesis, Mechanisms and Applications, Renewable and Sustainable Energy Reviews, Vol. 81, 2018, pp. 536-551, https://doi.org/10.1016/j.rser.2017.08.020.

[40] C. Van, H. Nguyen, H. Huynh, H. Pham, T. Dinh, H. Luong, B. Phan, C. Tran, V. Dang, Multi-modification of ZnO Nanorods to Enhance the Visible Absorption, Advances in Natural Sciences: Nanoscience and Nanotechnology, Vol. 11, No. 1, 2020, pp. 015002, https://doi.org/10.1088/2043-6254/ab6290.

[41] H. N. Pham, M. H. Tong, H. Q. Huynh, H. D. Phan, C. K. Tran, B. T. Phan, V. Q. Dang, The Enhancement of Visible Photodetector Performance based on Mn-doped ZnO Nanorods by Substrate Architecting, Sensors and Actuators A: Physical, Vol. 311, 2020, pp. 112085, https://doi.org/10.1016/j.sna.2020.112085.